Research Article | Vol. 28, No. 8 / 13 April 2020 / Optics Express 12201
Optics EXPRESS

Continuous-wave electrically injected GaN-on-Si microdisk laser diodes

JIN WANG,[1,2] MEIXIN FENG,[2,3,6] RUI ZHOU,[2,4] QIAN SUN,[2,3,4,7] JIANXUN LIU,[2] XIUJIAN SUN,[2] XINHE ZHENG,[1,8] MASAO IKEDA,[2] XING SHENG,[5] AND HUI YANG[2,4]

[1]*University of Science and Technology Beijing, Beijing 100083, China*
[2]*Key Laboratory of Nano-Devices and Applications, Suzhou Institute of Nano-Tech and Nano-Bionics, Chinese Academy of Sciences (CAS), Suzhou 215123, China*
[3]*Suzhou Institute of Nano-Tech and Nano-Bionics, CAS, Foshan 528200, China*
[4]*University of Science and Technology of China, Hefei 230026, China*
[5]*Department of Electronic Engineering, Tsinghua University, Beijing 100084, China*
[6]*mxfeng2011@sinano.ac.cn*
[7]*qsun2011@sinano.ac.cn*
[8]*xinhezheng@ustb.edu.cn*

Abstract: Silicon photonics has been calling for an electrically pumped on-chip light source at room temperature for decades. A GaN-based microdisk laser diode with whispering gallery modes grown on Si is a promising candidate for compact on-chip light source. By suppressing the unintentional incorporation of carbon impurity in the p-type AlGaN cladding layer of the laser, we have significantly reduced the operation voltage and threshold current of the GaN-on-Si microdisk laser. Meanwhile the radius of the microdisk laser was shrunk to 8 μm to lower the thermal power. The overall junction temperature of the microdisk laser was effectively reduced. As a result, the first continuous-wave electrically pumped InGaN-based microdisk laser grown on Si was achieved at room temperature.

1. Introduction

GaN-based whispering-gallery mode (WGM) optical resonators have the advantages of low threshold current (I_{th}), small mode volumes and high quality factors, and can be widely used in various fields, including optical storage, and chemical and biological sensing, etc., [1–4]. Moreover, the light output of the microdisk laser can be easily coupled through an on-chip waveguide directly and efficiently [5–10], which enables the GaN-on-Si microdisk laser to serve as an alternative on-chip light source for Si-based optoelectronic integration by using III-nitride waveguide [11–13]. In addition, GaN-on-Si microdisk laser diodes can also be adopted in visible light communication [14–16]. Therefore, an electrically pumped GaN-based microdisk laser grown on Si has been pursued for over a decade.

However, only optically pumped lasing has been realized for most of the reported GaN-based microdisk lasers on Si, which is mainly due to the conventional "mushroom-like" architecture with an undercut structure. This kind of structure is indeed propitious for optically pumped lasing due to large optical confinement by using air as the cladding layer, but it also has many challenges for electrically pumped lasing [17–21]. For the microdisk laser with an undercut structure, electrical current cannot be injected through the air gap below the disk, but through the AlN/AlGaN multilayer buffer with a high resistivity between the active region and Si substrate, leading to a very large voltage [22]. The heat generated at the periphery of the microdisk cannot dissipate efficiently to the Si substrate because of the air gap, causing a huge thermal resistance and high junction temperature.

#391851 https://doi.org/10.1364/OE.391851
Journal © 2020 Received 3 Mar 2020; revised 2 Apr 2020; accepted 4 Apr 2020; published 8 Apr 2020

Optics EXPRESS

In our previous work, we proposed a "sandwich-like" architecture with AlGaN cladding layers on both sides of the quantum wells to reduce the electrical series resistance and thermal resistance, which resulted in the first demonstration of electrically pumped (in a pulsed mode) GaN-based microdisk laser grown on Si at room temperature with a radius of 20 μm. But the I_{th} and threshold voltage of the GaN-on-Si microdisk laser were 240 mA and about 8 V [4], respectively, which were relatively high as compared with the reported GaN-based lasers with a Fabry–Pérot cavity. High threshold current and threshold voltage induced lots of joule heat and a high junction temperature, which prevented the device from continuous-wave (CW) operation. On the other hand, the chip size of the as-fabricated GaN-on-Si microdisk laser was too large, as compared with GaAs-based microdisk lasers, which led to a large mode volume and high power consumption, hindering its adoption for on-chip integration.

In an electrically pumped microdisk laser structure, a p-type cladding layer is required not only to confine the optical field in the active region, but also to provide holes to multi-quantum wells (MQWs) for recombination with electron to generate photons. It is reported that the proportion of the optical field distribution in the p-type cladding layer is relatively high (~30%), and the absorption coefficient of p-type cladding layer is much larger than that of other layers [23,24], because of the presence of Mg acceptors [25–27] and the deep level defect formed by the unintentionally incorporated carbon (C) impurities in p-type layer [28,29]. Meanwhile, C impurities also often act as compensation centers for the holes in the p-type cladding layer, increasing the series resistance. In order to reduce the operation junction temperature and realize CW lasing for GaN-on-Si microdisk laser diodes, we studied and effectively suppressed the unintentional incorporation of carbon impurities in the p-type cladding layer, which significantly reduced the series resistance and optical loss, leading to a further decrease of operation voltage and threshold current, and hence joule heat generation. Also we shrank the microdisk radius to 8 μm to further ameliorate the thermal power. As a result, we realized the first CW operation of room-temperature electrically pumped GaN-based microdisk laser diodes grown on Si substrate.

2. Experiment

Decreasing the C concentration in the p-type cladding layer is an effective method to reduce both the series resistance and optical loss, which further leads to the decrease of operation voltage and threshold current [23]. Two microdisk laser samples, named as samples A and B, were prepared to study the influence of C impurity concentration in p-type cladding layers. These two samples were overgrown on the n-GaN template grown on Si substrates by metal organic chemical vapor deposition, including optical cladding layers, waveguide layers, active region, electron blocking layer, and contact layer, as shown in Fig. 1(a). The detailed information can be found in our previous work [4]. The only difference between these two samples was the growth rate of p-type GaN/AlGaN superlattice cladding layer, which greatly affected the unintentional incorporation of C impurity. The growth rates of the p-type cladding layer of samples A and B were 17.4 and 8.7 nm/min, and their corresponding C concentrations were 2×10^{18} and 2×10^{17} cm^{-3} according to the secondary ion mass spectroscopy (SIMS) measurements, respectively. After device fabrication process [4], current-voltage (*I-V*) and light output power-current (*P-I*) characteristics of these two microdisk laser samples were measured under both CW and pulse (pulse width of 400 ns and the frequency of 10 kHz) modes.

For the microdisk laser with a radius of less than 20 μm, it is inconvenient to put the probe pin directly on the p-pad of the device. Therefore, we adopted an air-bridge electrode structure to enlarge the metal area as illustrated in Fig. 1(a) [30]. The size of the square metal pad was 100×100 μm^2, which was feasible for electrical testing by a probe pin. As shown in the scanning electron microscope (SEM) image shown in Fig. 1(b), the air-bridge structure was stable and uniform.

Optics EXPRESS

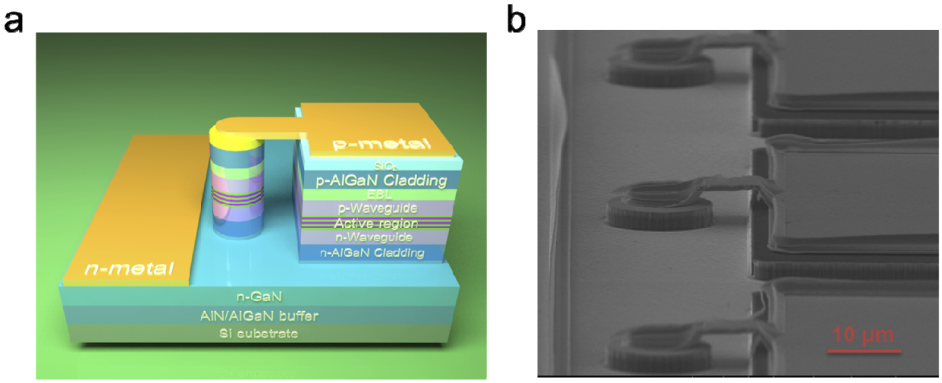

Fig. 1. (a) Schematic diagram of a GaN-based microdisk laser grown on Si with an air-bridge electrode structure, (b) bird-view SEM image of an array of microdisk laser diodes with a radius of 8 μm.

To enhance heat dissipation and reduce the junction temperature, the two laser samples were packaged on copper heat sink with indium soldering. The forward-voltage method was used to measure the junction temperature and thermal resistance of the devices. The principle of the forward-voltage method is based on the linear relationship between the junction temperature and the forward voltage of the LD under a small current injection. There are two states, the operation state with a normally high current injection and the measurement state with a very small current injection. The as-fabricated microdisk laser was firstly operated under a high current injection for a period of time to reach a steady junction temperature, and then quickly switched to the measurement state with a very small current injection. The current and voltage under the measurement state were recorded to indicate the change of the junction temperature. Because the injection current at the measurement state is so small that the induced thermal effect can be neglected, and the final junction temperature of the device under the measurement state will be equal to the ambient temperature after a long time. The switching time from the operation state to the measurement state is so short (about 100 ns) that it can be ignored. Therefore, the junction temperature at the beginning of the measurement state would be nearly equal to the value under the operation state, and the voltage change at the measurement state is caused by the junction temperature drop from the value of operation state to the ambient temperature. According to the near-linear relationship between the forward voltage and junction temperature under a small current injection, the junction temperature and thermal resistance of the microdisk laser can be obtained. A more detailed description and explanation of this method can be found in [31].

3. Results and discussion

Although increasing the growth temperature can reduce the C incorporation, the InGaN-based active region may be degraded during the growth of p-type cladding layer at high temperature. Therefore, we reduced the growth rate of p-type AlGaN cladding layer to achieve a lower C incorporation, without causing significant degradation of the active region. When slowing down the growth rate, the flow rates of Ga and Al sources were reduced, and these precursors were the main source of C impurity. Meanwhile, the reduction of these precursor flow rates led to an effectively higher V/III ratio. As a result, the unintentional incorporation of C impurities in sample B was reduced by an order of magnitude, as compared with that of sample A.

We firstly fabricated the top-ring-contact microdisk lasers from these two epitaxial structures, and the top-ring-contact microdisk lasers contained an inner current blocking circle with a SiO_2 insulation layer underneath, as shown in Fig. 2(a). The radius of outer and inner circles of the

Optics EXPRESS

device were 20 and 10 μm, respectively. As shown in Fig. 2(b), the operation voltage at 50 mA deceased from 7 (sample A) to 5.9 V (sample B), and the corresponding series resistance at 50 mA was reduced from 65 to 49 Ω. This result confirmed that the effective suppression of unintentional incorporation of C impurities in the 500-nm-thick p-type cladding layer can greatly reduce the electrical compensation and series resistance, contributing to a much lower operation voltage and junction temperature. On the other hand, according to the *L-I* curves of these two samples shown in Fig. 2(c), the threshold current of the microdisk laser was reduced from 240 (sample A) to 60 mA (sample B) because of the reduction of the C concentration in the p-type cladding layer. The deep level defect formed by the unintentionally incorporated C impurities in p-type cladding layer can induce optical loss, so sample B with a lower C concentration had a reduced optical loss and lower threshold current. Thanks to the reduced optical loss and junction temperature, the slope efficiency of sample B was much larger than that of sample A (Fig. 2(c)). It is noted that the *P-I* curve of sample A tended to saturate when the injection current increased beyond 300 mA, indicating a slope efficiency droop, which was mainly induced by the self-heating effect because of the relatively high operation voltage and threshold current. For sample B with a much lower operation voltage and threshold current, the slope efficiency maintained a high value beyond the threshold, reflecting a much reduced junction temperature, as compared to that of sample A.

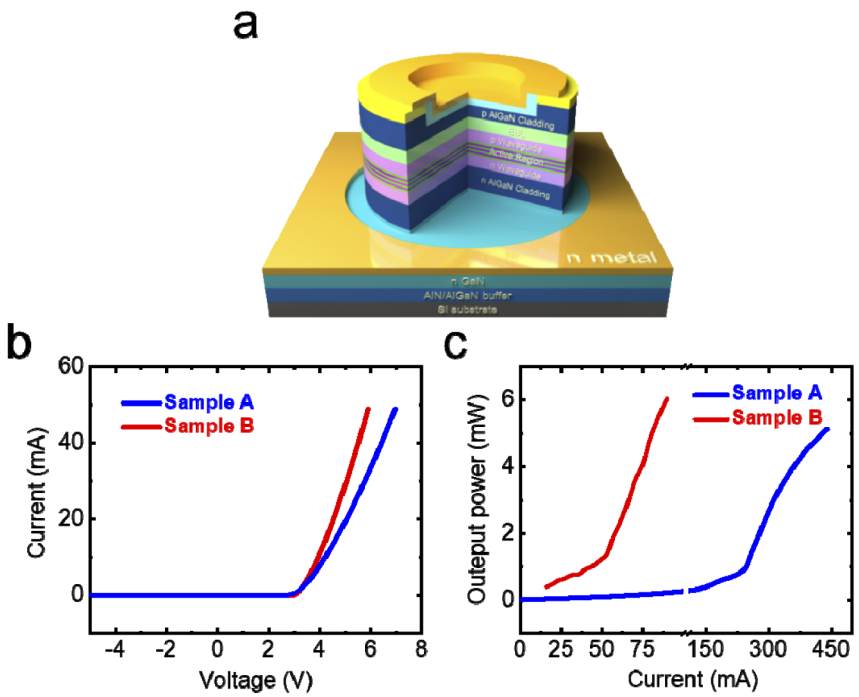

Fig. 2. (a) The schematic diagram of top-ring-contact microdisk laser structure, (b) *I-V* curves and (c) *P-I* characteristics of top-ring-contact microdisk laser samples A and B, respectively.

To illustrate the effect of the improvements in threshold current and operation voltage, we estimated the junction temperature of the two microdisk laser samples. The junction temperature is described by the equation, $\Delta T = P_{th} \cdot R_{th}$, where P_{th} and R_{th} are the thermal power and thermal resistance, respectively. Before lasing, the spontaneous optical power is very small, and the thermal power P_{th} is nearly equal to the injected electric power P_{inj}. Hence the P_{inj} can be

Optics EXPRESS

determined by the product of the current and voltage, and R_{th} can be measured by the forward-voltage method. Figure 3(a) shows the relationship between the current and voltage of sample B after switching from the operation state with an injection current of 50 mA to the measurement state with a low injection of about 0.35 mA. After approximately 20 μs, the voltage and current reached a steady state, and the junction temperature of the device was almost equal to the ambient temperature due to the efficient heat dissipation through package. The voltage change in Fig. 3(a) was 95 mV. The relation between the junction temperature and the forward voltage at a small current of 0.35 mA was shown in Fig. 3(b). The solid dots and lines represented the experimental data and their linear fitting, respevtively. The measured temperature coefficient of sample B was -2.55 mV/K, and the junction temperature rise at the injection current of 50 mA was 37 °C, and the thermal resistance was calculated to be 126 K/W. The thermal resistance of sample A (121 K/W) was also measured by the same method, which was close to that of sample B since the both samples had the same structure and package. Prior to lasing, the thermal power P_{th} can be estimated by the injected electric power P_{inj} determined by the product of the voltage and threshold current (Fig. 2), the estimated junction temperature of samples A and B to realize electrically injected CW lasing were over 200 and about 50 °C, respectively. The striking difference in juction temperature of the top-ring-contact microdisk laser diodes mainly came from great suppression of unintentional incorporation of C impurities in the p-type cladding layer.

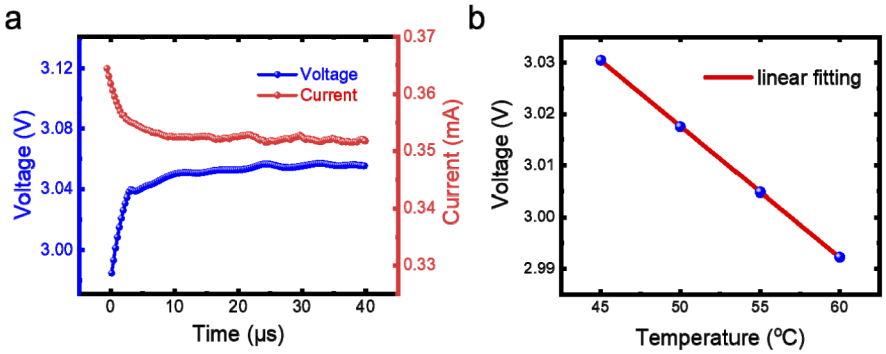

Fig. 3. (a) The current and voltage of the device after switching from the operation state to the measurement state, (b) the relation between the junction temperature and the forward voltage at a small injection current of 0.35 mA for sample B.

Another way to further reduce the heat generation at threshold of the device is to shrink the device size. To study the effect of device size on the threshold current, we fabricated microdisk laser diodes with various radius from the epitaxial structure of sample B. The threshold current of the as-fabricated microdisk laser diodes were measured in a pulsed mode. The threshold current decreased from 100 to 15 mA with the radius of the microdisk reduced from 20 to 8 μm, indicating that the injected electrical power at threshold reduced with the decreasing radius of the devices in the range under discussion. According to the equation, $\Delta T = P_{inj} \cdot R_{th}$, though the thermal resistance of device increased with shrinking the device size, meanwhile, the significant reduction of injected electrical power at threshold may plays a more important role and leading to a lower junction temperature at threshold, which is contributing to the CW lasing operation. The testing results in CW mode show that microdisk lasers with a radius of 20 μm cannot lase (not shown here) and the devices with a radius of 8 μm can lase, which proves the discussion above.

Figure 4(a) shows the electroluminescence (*EL*) spectra of one microdisk laser with a radius of 8 μm fabricated from the epitaxial structure of sample B under various CW current injection. A broad spontaneous emission peaked around 407 nm was obtained under a small CW current

Optics EXPRESS

injection. But with the injection current exceeded 18 mA, a stimulated emission at 410 nm was observed. Figure 4(b) shows the variation of the FWHM of the *EL* spectra and the *EL* output power as a function of the CW injection current. The slope of the *P-I* curve increased abruptly with a distinct discontinuity after the injection current exceeded 18 mA, and meanwhile the FWHM of the emission spectrum quickly narrowed down to 0.5 nm, both of which concluded that a CW lasing operation of the as-fabricated microdisk laser grown on Si with a threshold current of 18 mA was achieved at room temperature. The threshold current of 18 mA for CW operation was just a little higher than that of 15 mA for pulsed injection, indicating that the influence of self-heating on the device performance was greatly suppressed because of the improved epitaxial structure and reduced microdisk size.

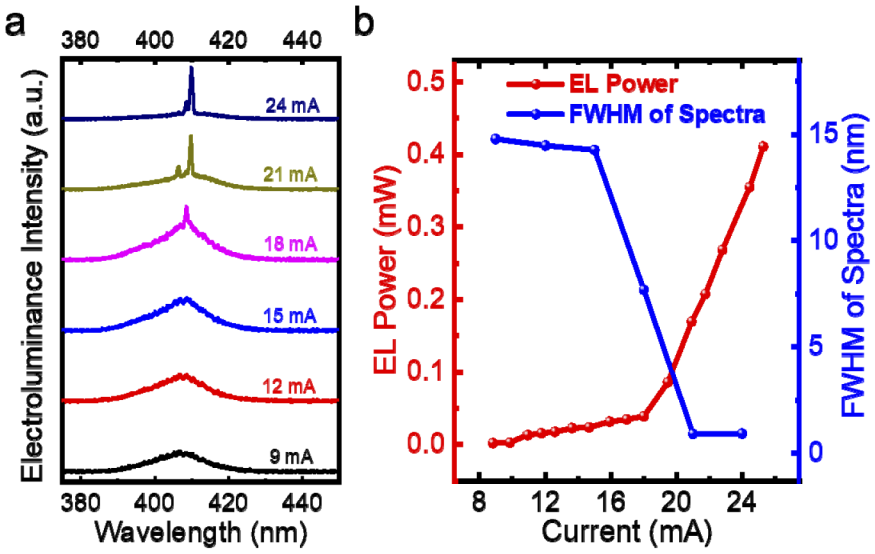

Fig. 4. (a) EL spectra of the microdisk laser diode with a radius of 8 μm measured under various CW current injection. (b) FWHM of the EL spectra and EL output power as a function of the CW injection current.

4. Conclusion

In summary, with the reduction of the growth rate of p-AlGaN cladding layer in the microdisk laser epitaxial structure, the unintentional incorporation of C impurities in the p-type cladding layer was effectively suppressed by one order of magnitude. As a result, both the operation voltage and threshold current of the microdisk laser greatly decreased, leading to a lower junction temperature at threshold, because of the reduction of the series resistance and optical loss. Furthermore, the improved laser epitaxial structure combined with reduced microdisk dimension (8 μm in radius) dramatically lowered the thermal power and junction temperature at threshold, which led to the CW operation of electrically pumped GaN-based microdisk lasers grown on Si with a threshold current of 18 mA at room temperature. Research to further decrease the threshold current of the GaN-on-Si microdisk lasers is underway by both improving the epitaxial material quality and applying top-ring-contact microdisk device structure to the small-size microdisk with more advanced patterning technique.

Optics EXPRESS

Funding

Key-Area Research and Development Program of GuangDong Province (2019B010130001, 2019B090917005); National Key Research and Development Program of China (2016YFB0400100, 2016YFB0400104,2018YFA0703702); National Natural Science Foundation of China (61534007, 61775230, 61804162, 61874131); Chinese Academy of Sciences (QYZDB-SSW-JSC014,ZDBS-LY-JSC040); Jiangsu Provincial Key Research and Development Program (BE2017079); Natural Science Foundation of Jiangsu Province (BK20180253); Suzhou Science and Technology Program (SYG201846, SYG201927); China Postdoctoral Science Foundation (2018M632408); Open Fund of the State Key Laboratory of Reliability and Intelligence of Electrical Equipment (EERIKF2018001).

Acknowledgments

We are thankful for the technical support from Nano Fabrication Facility, Platform for Characterization & Test, and Nano-X of SINANO, CAS.

Disclosures

The authors declare that they have no conflict of interest.

References

1. K. J. Vahala, "Optical microcavities," Nature **424**(6950), 839–846 (2003).
2. A. C. Tamboli, E. D. Haberer, R. Sharma, K. Lee, S. Nakamura, and E. L. Hu, "Room-temperature continuous-wave lasing in GaN/InGaN microdisks," Nat. Photonics **1**(1), 61–64 (2007).
3. Y. Wan, J. Norman, Q. Li, M. Kennedy, D. Liang, C. Zhang, D. Huang, Z. Zhang, A. Y. Liu, A. Torres, D. Jung, A. C. Gossard, E. L. Hu, K. M. Lau, and J. E. Bowers, "1.3 μm submilliamp threshold quantum dot micro-lasers on Si," Optica **4**(8), 940–944 (2017).
4. M. Feng, J. He, Q. Sun, H. Gao, Z. Li, Y. Zhou, J. Liu, S. Zhang, D. Li, L. Zhang, X. Sun, D. Li, H. Wang, M. Ikeda, R. Wang, and H. Yang, "Room-temperature electrically pumped InGaN-based microdisk laser grown on Si," Opt. Express **26**(4), 5043–5051 (2018).
5. Y. Sun, K. Zhou, Q. Sun, J. P. Liu, M. X. Feng, Z. C. Li, Y. Zhou, L. Q. Zhang, D. Y. Li, S. M. Zhang, M. Ikeda, S. Liu, and H. Yang, "Room-temperature continuous-wave electrically injected InGaN-based laser directly grown on Si," Nat. Photonics **10**(9), 595–599 (2016).
6. Y. Sun, K. Zhou, M. X. Feng, Z. C. Li, Y. Zhou, Q. Sun, J. P. Liu, L. Q. Zhang, D. Y. Li, X. J. Sun, D. B. Li, S. M. Zhang, M. Ikeda, and H. Yang, "Room-temperature continuous-wave electrically pumped InGaN/GaN quantum well blue laser diode directly grown on Si," Light: Sci. Appl. **7**(1), 13 (2018).
7. M. X. Feng, Z. C. Li, J. Wang, R. Zhou, Q. Sun, X. J. Sun, D. B. Li, H. W. Gao, Y. Zhou, S. M. Zhang, D. Y. Li, L. Q. Zhang, J. P. Liu, H. B. Wang, M. Ikeda, X. H. Zheng, and H. Yang, "Room-temperature electrically injected AlGaN-based near-ultraviolet laser grown on Si," ACS Photonics **5**(3), 699–704 (2018).
8. M. X. Feng, J. Wang, R. Zhou, Q. Sun, H. W. Gao, Y. Zhou, J. X. Liu, Y. N. Huang, S. M. Zhang, M. Ikeda, H. B. Wang, Y. T. Zhang, Y. J. Wang, and H. Yang, "On-chip integration of GaN-based laser, modulator, and photodetector grown on Si," IEEE J. Sel. Top. Quantum Electron. **24**(6), 1–5 (2018).
9. Q. Sun, W. Yan, M. X. Feng, Z. C. Li, B. Feng, H. M. Zhao, and H. Yang, "GaN-on-Si blue/white LEDs: epitaxy, chip, and package," J. Semicond. **37**(4), 044006 (2016).
10. J. Wang, M. X. Feng, R. Zhou, Q. Sun, J. X. Liu, Y. N. Huang, Y. Zhou, H. W. Gao, X. H. Zheng, M. Ikeda, R. Huang, F. S. Li, A. Ding-Sun, and H. Yang, "The abnormal aging phenomena in GaN-based near-ultraviolet laser diodes," J. Phys. D: Appl. Phys. **52**(27), 275104 (2019).
11. F. Tabataba-Vakili, L. Doyennette, C. Brimont, T. Guillet, S. Rennesson, E. Frayssinet, B. Damilano, J. Duboz, F. Semond, I. Roland, M. E. Kurdi, X. Checoury, S. Sauvage, B. Gayral, and P. Boucaud, "Blue microlasers integrated on a photonic platform on silicon," ACS Photonics **5**(9), 3643–3648 (2018).
12. F. Tabataba-Vakili, L. Doyennette, C. Brimont, T. Guillet, S. Rennesson, B. Damilano, E. Frayssinet, J. Duboz, X. Checoury, S. Sauvage, M. E. Kurdi, F. Semond, B. Gayral, and P. Boucaud, "Demonstration of critical coupling in an active III-nitride microdisk photonic circuit on silicon," Sci. Rep. **9**(1), 18095 (2019).
13. Y. C. Yang, B. C. Zhu, Z. Shi, J. Y. Wang, X. Li, X. M. Gao, J. L. Yuan, Y. H. Li, Y. Jiang, and Y. J. Wang, "Multi-dimensional spatial light communication made with on-chip InGaN photonic integration," Opt. Mater. **66**, 659–663 (2017).
14. Y. Yang, B. Zhu, Z. Shi, J. Wang, X. Li, X. Gao, J. Yuan, Y. Li, Y. Jiang, and Y. Wang, "Multi-dimensional spatial light communication made with on-chip InGaN photonic integration," Opt. Mater. **66**(17), 659–663 (2017).

Optics EXPRESS

15. X. B. Sun, Z. Y. Zhang, A. Chaaban, T. K. Ng, C. Shen, R. Chen, J. C. Yan, H. D. Sun, X. H. Li, J. X. Wang, J. M. Li, M.-S. Alouini, and B. S. Ooi, "71-Mbit/s ultraviolet-B LED communication link based on 8-QAM-OFDM modulation," Opt. Express **25**(19), 23267–23274 (2017).
16. Z. Y. Xu and B. M. Sadler, "Ultraviolet communications potential and state-of-the-art," IEEE Commun. Mag. **46**(5), 67–73 (2008).
17. J. Sellés, V. Crepel, I. Roland, M. El Kurdi, X. Checoury, P. Boucaud, M. Mexis, M. Leroux, B. Damilano, S. Rennesson, F. Semond, B. Gayral, C. Brimont, and T. Guillet, "III-Nitride-on-silicon microdisk lasers from the blue to the deep ultra-violet," Appl. Phys. Lett. **109**(23), 231101 (2016).
18. M. Athanasiou, R. Smith, B. Liu, and T. Wang, "Room temperature continuous-wave green lasing from an InGaN microdisk on silicon," Sci. Rep. **4**(1), 7250 (2015).
19. H. W. Choi, K. N. Hui, P. T. Lai, P. Chen, X. H. Zhang, S. Tripathy, J. H. Teng, and S. J. Chua, "Lasing in GaN microdisks pivoted on Si," Appl. Phys. Lett. **89**(21), 211101 (2006).
20. S. Vicknesh, S. Tripathy, V. K. X. Lin, L. S. Wang, and S. J. Chua, "Fabrication of deeply undercut GaN-based microdisk structures on silicon platforms," Appl. Phys. Lett. **90**(7), 071906 (2007).
21. X. Liu, W. Fang, Y. Huang, X. H. Wu, S. T. Ho, H. Cao, and R. P. H. Chang, "Optically pumped ultraviolet microdisk laser on a silicon substrate," Appl. Phys. Lett. **84**(14), 2488–2490 (2004).
22. D. Visalli, M. V. Hove, M. Leys, J. Derluyn, E. Simoen, P. Srivastava, K. Geens, S. Degroote, M. Germain, A. P. D. Nguyen, A. Stesmans, and G. Borghs, "Investigation of Light-Induced Deep-Level Defect Activation at the AlN/Si Interface," Appl. Phys. Express **4**(9), 094101 (2011).
23. C. Y. Huang, Y. D. Lin, A. Tyagi, A. Chakraborty, H. Ohta, J. S. Speck, S. P. DenBaars, and S. Nakamura, "Optical waveguide simulations for the optimization of InGaN-based green laser diodes," J. Appl. Phys. **107**(2), 023101 (2010).
24. L. Q. Zhang, D. S. Jiang, J. J. Zhu, D. G. Zhao, Z. S. Liu, S. M. Zhang, and H. Yang, "Confinement factor and absorption loss of AlInGaN based laser diodes emitting from ultraviolet to green," J. Appl. Phys. **105**(2), 023104 (2009).
25. J. K. Son, S. N. Lee, H. S. Paek, T. Sskong, H. K. Kim, Y. Park, H. Y. Ryu, O. H. Nam, J. S. Hwang, and Y. H. Cho, "Measurement of optical loss variation on thickness of InGaN optical confinement layers of blue-violet-emitting laser diodes," J. Appl. Phys. **103**(10), 103101 (2008).
26. D. Sizov, R. Bhat, and C. E. Zah, "Optical absorption of Mg-doped layers and InGaN quantum wells on c-plane and semipolar GaN structures," J. Appl. Phys. **113**(20), 203108 (2013).
27. M. Martens, C. Kuhn, T. Simoneit, S. Hagedorn, A. Knauer, T. Wernicke, M. Weyers, and M. Kneissl, "The effects of magnesium doping on the modal loss in AlGaN-based deep UV lasers," Appl. Phys. Lett. **110**(8), 081103 (2017).
28. J. D. Ye, S. L. Gu, L. Z. Wang, R. Zhang, Y. Shi, and Y. D. Zheng, "Optical Characteristics of C-Doped GaN," Chin. J. Semicond. **23**(7), 717–721 (2002).
29. J. X. Liu, J. Wang, X. J. Sun, M. X. Feng, X. T. Ge, J. Q. Ning, R. Zhou, Y. Zhou, H. W. Gao, M. Ikeda, and H. Yang, "Performance improvement of InGaN-based laser grown on Si by suppressing point defects," Opt. Express **27**(18), 25943–25952 (2019).
30. J. Wang, M. X. Feng, R. Zhou, Q. Sun, J. X. Liu, Y. N. Huang, Y. Zhou, H. W. Gao, X. H. Zheng, M. Ikeda, and H. Yang, "GaN-based ultraviolet microdisk laser diode grown on Si," Photonics Res. **7**(6), B32–B35 (2019).
31. P. Y. Wen, D. Y. Li, S. M. Zhang, J. P. Liu, L. Q. Zhang, K. Zhou, M. X. Feng, Z. C. Li, A. Q. Tian, and H. Yang, "High accuracy thermal resistance measurement in GaN/InGaN laser diodes," Solid-State Electron. **106**, 50–53 (2015).